Journal of Applied Polymer Science

Synthesis and characterization of multi-hollow opaque polymer pigments

Serdar Asmaoğlu,[1] Güngör Gündüz,[1] Bora Maviş,[2] Üner Çolak[3]
[1]Kimya Mühendisliği Bölümü, Orta Doğu Teknik Üniversitesi, Ankara 06800, Turkey
[2]Makina Mühendisliği Bölümü, Hacettepe Üniversitesi, Ankara 06800, Turkey
[3]Nükleer Enerji Mühendisliği Bölümü, Hacettepe Üniversitesi, Ankara 06800, Turkey
Correspondence to: G. Gündüz (E-mail: ggunduz@metu.edu)

ABSTRACT: A new generation multihollow opaque polymer pigment was synthesized by suspension polymerization of "water-in-oil-in-water" emulsion method, where methyl methacrylate and ethylene glycol dimethacrylate monomer mixture was used as oil phase. The effects of surfactant and cosurfactant composition in terms of "hydrophilic/lipophilic balance" on the stability of the "water-in-oil" emulsion and the size of water droplets were studied. Low droplet sizes and the optimum stability were obtained with "Span 80&Tween 80" surfactant mixture at an HLB value of 8. The desired size distribution was obtained at "monomer/surfactant/water" ratio of 75.5/9.4/15.1 at an ultrasonic mixing power of 80 W lasting for 30 s. The surface morphology and hollow structure of polymer pigments were analyzed by scanning and transmission electron microscopy techniques. L^*a^*b color and gloss properties of polymer pigments were examined. The opacity values were assessed by contrast ratio measurements, and the pigments provided up to 97.3% opacity with 50% v/v solid content in resin. In addition, the pigments exhibited low gloss values and yielded matte films.
 J. Appl. Polym. Sci. **2016**, *133*, 43696.

KEYWORDS: coatings; dyes/pigments; emulsion polymerization; morphology; optical properties

Received 5 January 2016; accepted 26 March 2016
DOI: 10.1002/app.43696

INTRODUCTION

Pigments are used as colorants and fillers in many materials such as paints, cosmetics, and polymers. Most of the white pigments and extenders used in paint industry are inorganic substances like calcite, titanium dioxide, zinc sulfide, zinc oxide, and baryte. The incompatibility between inorganic pigments and organic resins causes severe paint defects and may result in phase separation, agglomeration, or settling. The high density difference between organic vehicle and inorganic pigments is another source of such defects.

In the last decade, the hollow polymer particles have received significant attention with their lower density and high compatibility with organic paint resins, and so have become better options as opaque polymer pigments to traditional white pigments. Opaque polymer pigments have a structure with thin polymeric shell and a single void inside.[1–4] When an incident beam of electromagnetic radiation within the visible region interacts with a particle having diameter close to the wavelength of radiation, the particle scatters radiation nonselectively. Opaque pigments provide white appearance and opacity because of scattering of light randomly at all angles. The mathematical analysis of light scattering from small particles for a real case was first described by Mie,[5,6] and then, Bohren and Huffman[6] revised the Mie scattering for spherical particles. The scattering efficiency is dependent on the shape and size of particle, the refractive index difference between medium and particle, the wavelength of light, and the number of particles which act as scattering centers.[2,7,8] In contrast to traditional pigments, the scattering centers in opaque polymer pigments are voids instead of particles.

Void structured spherical polymer particles were first produced by Kowalski and Vogel and patented in 1984.[9,10] Thereafter, the studies were focused on optimizing these particles to use them as opacifying agent and it was first commercialized by Rohm & Haas Co. Commercialized polymer pigments are mainly produced by osmotic swelling. In this method, low molecular weight oligomers containing carboxylic acid groups are encapsulated by shell polymers. With alkali addition, the acid groups neutralize and polyelectrolytes form. The increased inner osmotic pressure due to electrolytes leads to the absorption of water which in turn causes swelling.[2,11,12]

The purpose of this present study is to produce a new generation opaque polymer pigment with multihollow structure to be

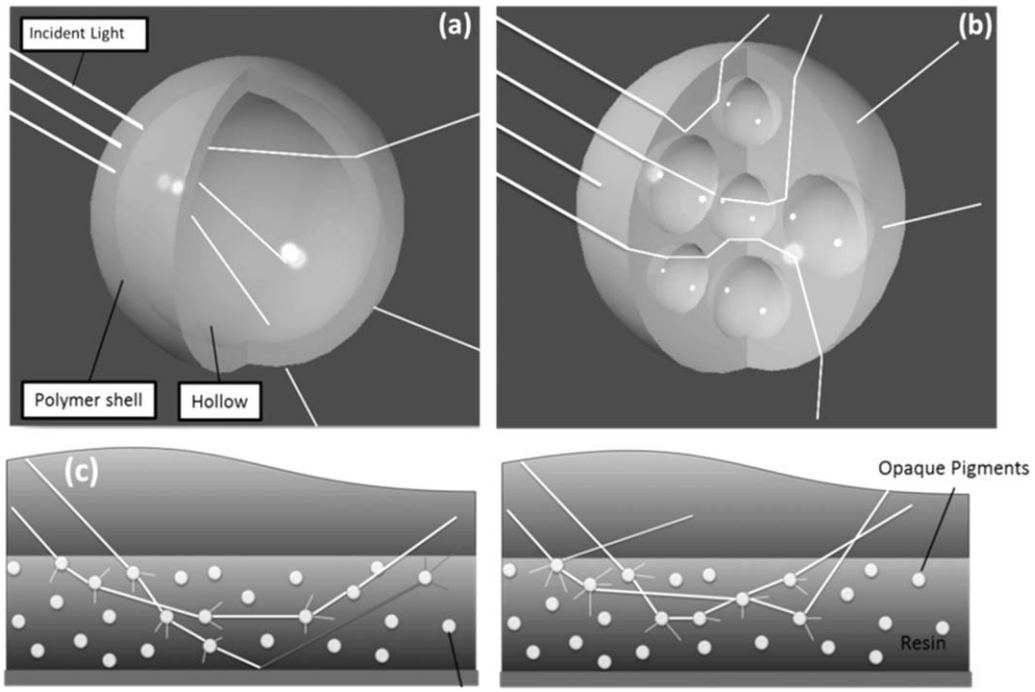

Figure 1. Illustration of (a) single-hollow, (b) multihollow polymer pigment, and (c) the mechanism of the improvement of hiding efficiency.

used in surface coating. The increase in the number of hollows inside polymer particles can enhance the scattering efficiency and thus may impart higher opacity and hiding power than single-hollow particles. The illustration for the intended structure to be made is given in Figure 1b.

In this work, multihollow structured polymer particles were produced by suspension polymerization of "water-in-oil-in-water (W/O/W) emulsion" system. "Oil" means "monomer" throughout the text. The W/O/W emulsions can be produced by dispersing "water-in-oil" (W/O) emulsions in continuous water phase which contains hydrophilic surfactant.[13–15] In W/O emulsions, water droplets are dispersed in monomer phase inside the spherical micelles by using a hydrophobic surfactant. High speed mixing and ultrasonication are needed to make fine W/O emulsions. The size of hollows inside particles are theoretically equivalent to the size of water droplets formed in W/O emulsification step. W/O/W emulsions are mainly used in controlled drug delivery systems, food industry, and cosmetics.[16–18]

Emulsion stability is a key factor for producing multihollow structured particles by W/O/W emulsion polymerization. The nature of monomer phase, diameter of water droplets, type and structure of surfactants, viscosity of monomer, and the density difference between water and monomer directly affect the stability.[19–22] Creaming, sedimentation, flocculation, coalescence, phase inversion, and Oswald ripening are the mechanisms of emulsion destabilization. Sedimentation occurs when the monomer density is lower than water density and creaming occurs in reverse.[22] Coalescence and flocculation are caused by droplet aggregation and migration.[22] Phase inversion is the change of W/O emulsion to O/W emulsion, and vice versa, with the change of temperature of the medium[23–25] or with the increase of dispersed phase volume (here water) is beyond a critical value.[25,26] The illustration for instability mechanisms is given in Figure 2.

Small droplets have higher "Laplace pressure" due to high curvature.[27,28] The Oswald ripening is the fusion of smaller droplets into bigger droplets because of the Laplace pressure difference.[22,24] It is not easy to produce submicron sized hollows because of the high Laplacian pressure due to high curvature, which, leads to destabilization of the emulsion easily. In order to increase emulsion stability and preserve inner water droplets during polymerization, a cosurfactant in W/O emulsion and thickening agent in monomer phase were used in this research. It was already stated in various studies that the use of cosurfactant in W/O emulsion enhanced the stability.[24,29,30] The required ratio of surfactants can be predicted from "hydrophilic-lipophilic balance" (HLB) value. The HLB value is a scale which relates the percentage of hydrophilic to lipophilic groups in the surfactant(s).[31,32]

In this work, W/O emulsions were prepared by using Span 80-Tween 80 surfactant mixtures through utrasonication. The effect of HLB number and sonication parameters on emulsion stability and size were investigated. The stable region for W/O emulsion was determined on a ternary phase diagram. The size of water droplet needed to achieve maximum scattering efficiency was predicted by a mathematical model of the Mie scattering by using the Bohren and Huffman's formulation. The effect of mechanical mixing and hydrophilic surfactant concentration on the size of W/O/W emulsion droplets were studied, and the emulsions obtained were visually observed by optical microscopy. The W/O/W emulsions were then polymerized after stabilizing them in aqueous polyvinylpyrrolidone (PVP) aqueous solution. The morphological structure of the synthesized opaque polymer pigments were studied by using scanning electron

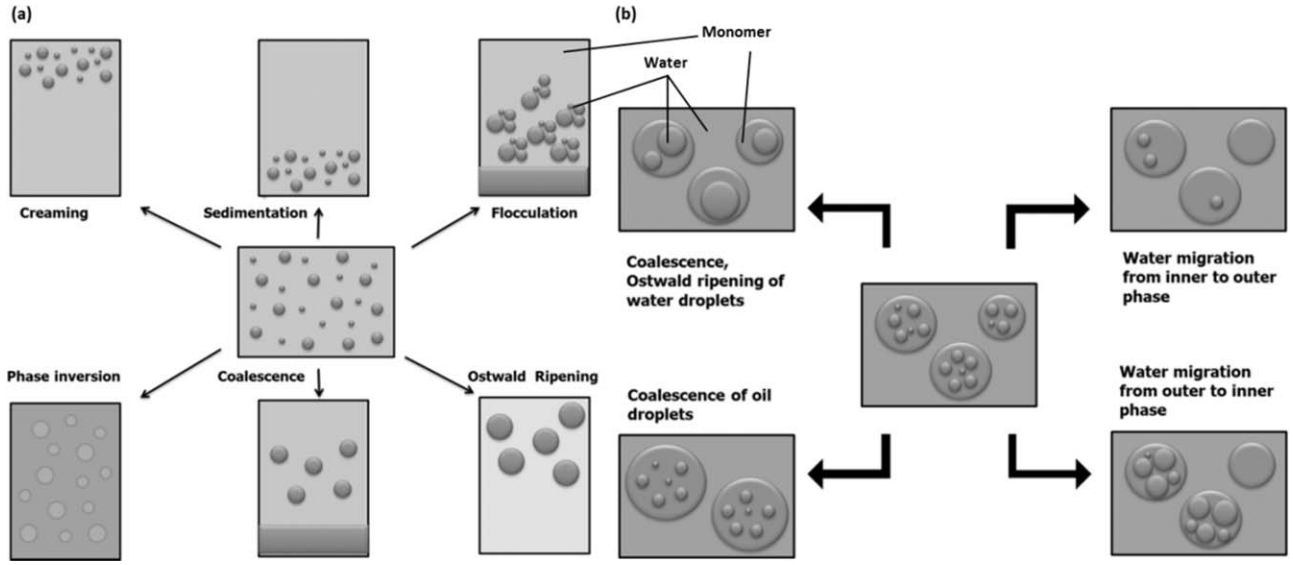

Figure 2. Instability mechanisms for (a) W/O and (b) W/O/W.

microscopy (SEM) and transmission electron microscopy (TEM). The opacity, the gloss, and the color properties of polymer pigments were investigated by using styrene-acrylic water based clear resin.

EXPERIMENTAL

Materials

The methyl methacrylate (MMA) and the crosslinking agent ethylene glycol dimethacrylate (EGDMA) (Merck, Germany) were used to synthesize the polymer. Lipophilic surfactant, Sorbitan monooleate (Span 80) (Sigma–Aldrich, Germany), and hydrophilic surfactant, polyoxyethylene (20) sorbitan monooleate (Tween 80) (Sigma–Aldrich, Germany), which have "hydrophilic-lipophilic balance value (HLB)" of 4.3, and 15, respectively, were used in the preparation of micelle particles in W/O emulsion. Polyoxyethylene (40) isooctylphenyl ether (Triton X-405) (Sigma–Aldrich, 70% in H_2O, HLB = 17.6) was the hydrophilic surfactant used in W/O/W multiple emulsion. The stabilizer polyvinylpyrrolidone (PVP) (MW = 1.3×10^6 g/mol), and the free radical initiator 2,2′azobisisobutyronitrile (AIBN) were purchased from Sigma–Aldrich (Germany).

Preparation of Water-in-Oil Emulsion

The W/O/W double emulsions were prepared by a procedure involving two steps. The first step is the preparation of W/O emulsion. First, a monomer mixture of 5 g MMA and 5 g EGDMA was prepared under magnetic stirring at 400 rpm for 15 min. Oil soluble free radical initiator (i.e., AIBN) was then added into the monomer mixture and dissolved by further mixing for 15 min. Then, the surfactant mixture of Span 80 and Tween 80 was added to the monomer mixture and dispersed for 30 min at 400 rpm by a magnetic stirrer. The composition of the binary mixture of Span 80 and Tween 80 mixture was estimated from their individual HLB values such that[31,32]

$$HLB_{\text{mix}} = x_1(HLB_1) + x_2(HLB_2), \quad (1)$$

where HLB_{mix} is the HLB value of surfactant mixture, x_1 is the weight fraction of surfactant 1, x_2 is the weight fraction of surfactant 2, $(HLB)_1$ is the HLB value of surfactant 1, and $(HLB)_2$ is the HLB value of surfactant 2.

After the preparation of monomer phase, distilled and deionized water was added to the mixture dropwise from a syringe. The amount of surfactant mixture and water used in the experiments was varied to investigate the stability and the size characteristics of W/O emulsions. The mixture was ultrasonically homogenized (Bandalin Sonopuls HD 2200; maximum power = 200 W). The sonication of mixtures was carried out in a cold water bath to avoid sudden temperature increase that may cause loss of components due to evaporation and also may cause emulsion instability. Milky white W/O emulsions were obtained after sonication.

Preparation of Water-in-Oil-in-Water Emulsion

The W/O emulsion thus prepared was then used to generate water-in-oil-in-water emulsion. The aqueous solution of Triton-X 405 was used as continuous phase of W/O/W emulsion. The Triton X-405 solution (60 g) with a concentration of 5% w/w (of total solution) was accomplished by mixing at 400 rpm for 2 h at ambient temperature. The W/O emulsion was slowly added into Triton-X 405 solution and agitated by a mechanical stirrer. The W/O/W emulsion thus obtained was milky white.

The W/O/W emulsion was stabilized by using 1% w/w aqueous solution of PVP by pouring the W/O/W emulsion slowly into PVP solution. It was added dropwise while mixing mechanically at 500 rpm. The illustration of W/O/W emulsion preparation steps is given in Figure 3.

Polymerization and Film Application

After the stabilization process, the emulsion was transferred into a four necked glass reactor equipped with a condenser and a temperature controller. Nitrogen was used to provide inert atmosphere over the liquid phase during polymerization. After the system was de-aerated, the reaction was carried out at 55 °C for 20 h. The reaction medium was mixed at 250 rpm during the entire process. Finally, solid opaque polymer pigments

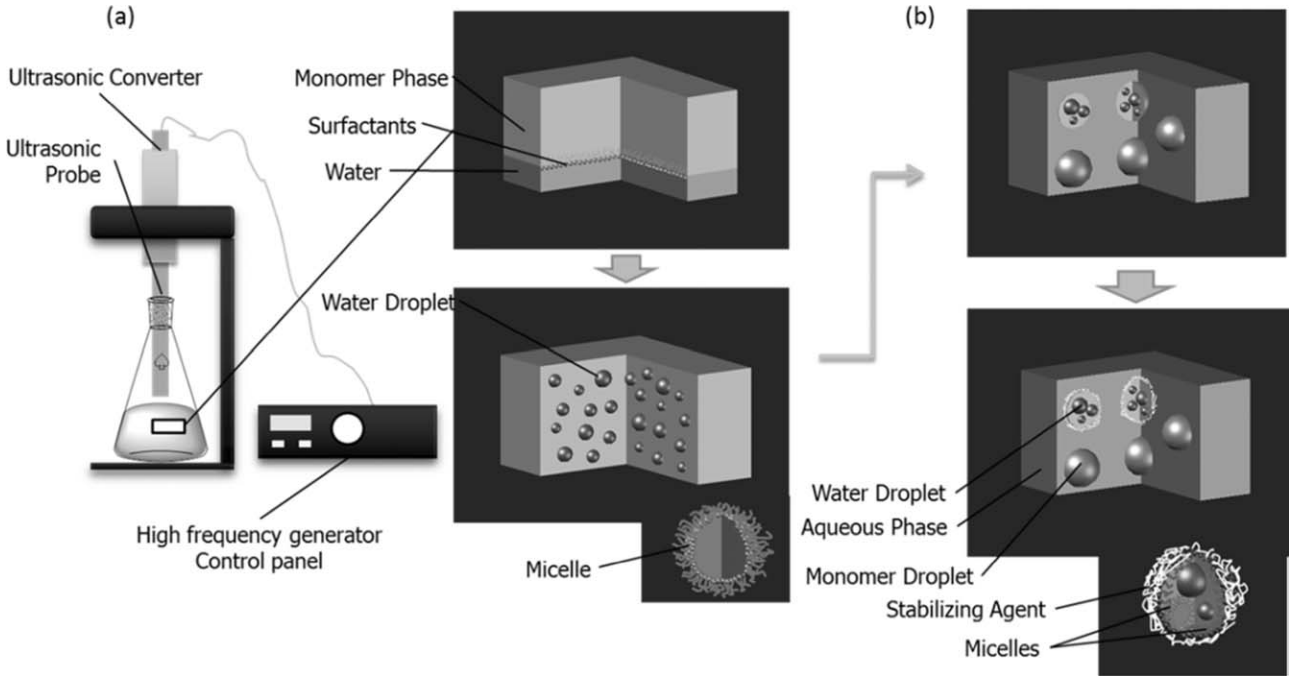

Figure 3. Flow diagram and illustration of (a) W/O emulsion and (b) W/O/W emulsion stabilization step.

dispersed in water was obtained. It was stable and phase separation did not occur in one week. However, some thickening occurred at the bottom due to the precipitation of larger particles. Anyway, the dispersion could be easily homogenized by agitation.

The opaque polymer pigments thus produced were mixed with a water-based styrene acrylic resin (Betapol SA-5017B, Betek Paint and Chemical Inc., Turkey) having up to 50% w/w pigment content in order to investigate the paint properties such as opacity and gloss.

The film applications were done by using an applicator at 150 μm wet thickness. All films were dried at ambient temperature for 24 h before test measurements.

Characterization Methods

The size of W/O and W/O/W emulsion samples were measured by Malvern Zetasizer Nano ZS (Model No: ZEN3500, $\lambda = 633$ nm laser) instrument. The W/O emulsion viscosity was determined using a vibrational viscometer (Model No: AND SV-10, constant frequency of 30 Hz).

The size and morphology of opaque polymer pigments were characterized by scanning electron microscopy (SEM) (Model: FEI Quanta 200 FEG). The polymer suspension was washed off twice using water-ethanol (1:1) mixture, and centrifuged. The samples were then vacuum (40 kPa) dried at 70 °C. The SEM specimens were coated with gold/palladium layer before the inspection.

The hollow structure of opaque polymer particles was investigated by using transmission electron microscopy (TEM) (Model: FEI Tecnai G2 Spirit, operated at 120 kV). The visual observation of emulsions was done by optical microscopy (Model: Prior, maximum magnification: ×1000).

The opacity measurements and color properties of the produced opaque polymer pigments were examined by using a color spectrophotometer (Model No: X-rite Color i5, spectral range: 360–750 nm, light source: CEI standard illuminant D65) and the gloss values of films were measured by using a glossmeter at incident angles of 20, 60, and 85° (Model: Rhopoint, Novo-Gloss).

RESULTS AND DISCUSSION

Preliminary Studies on Surfactant Selection

In order to prepare stable and submicron sized water-in-oil (W/O) emulsion, it is essential to select the appropriate surface active agent(s). For this purpose, first nonionic surfactants Span 80 (sorbitan monooleate, HLB = 4.3) and Span 83 (sorbitan sesquioleate, HLB = 3.7) both with lipophilic character were separately used, and the stability of prepared W/O emulsions was examined visually and also by size measurement. The surfactants were first dissolved in monomer(s) of methyl methacrylate (MMA) and/or ethylene glycol dimethacrylate (EGDMA), and water is then added into the solution. The preliminary experiments showed that Span 80-only and Span 83-only were not adequate to obtain homogeneous emulsions. After ultrasonic emulsification, very quick sedimentation and following phase separation was observed when each is used individually.

To create synergetic effect and to increase the interfacial film strength, a number of mixtures of Span 80-AOT (dioctyl sodium sulfosuccinate, HLB = 32), Span 80-Brij 97 (polyoxyethylene 10 oleoyl ether, HLB = 12), Span 80-SDBS (Sodium dodecylbenzenesulfonate, HLB = 11.7), Span 80-SLS (Sodium Lauryl Sulfate, HLB = 40), Span 83-Tween 80 [Polyoxyethylene (20) sorbitan monooleate, HLB = 15], and Span 80-Tween 80 were prepared and used for W/O emulsification. SDBS, AOT and SLS are anionic, and Brij 97 and Tween 80 are nonionic hydrophilic

Table I. Preliminary Experiments on Surfactant Selection

			Ratio of emulsion components			
Surfactant system	Monomer system	HLB	S	M	W	Stability observation
Span80	MMA:EGDMA(1:1)	4.3	6.2	73.7	20.1	Phase separation
Span80	MMA:EGDMA(1:1)	4.3	9.6	80.0	10.4	Sedimentation
Span80	MMA	4.3	10.0	80.0	10.0	Sedimentation
Span83	MMA:EGDMA(1:1)	3.7	10.0	80.0	10.0	Sedimentation
Span83	MMA:EGDMA(1:1)	3.7	6.9	80.0	13.1	Phase separation
Span80-AOT	MMA:EGDMA(1:1)	7	10.0	80.0	10.0	Phase separation
Span80-Brij97	MMA	7	9.8	78.4	11.8	Sedimentation

S, surfactant; M, monomer; W, water weight ratio.

surfactants. The surfactant (S), monomer (M), water (W) weight ratio, the HLB number of surfactant mixtures and the observed emulsion stability properties were given in Table I.

The emulsions which were homogenous and did not undergo phase separation or sedimentation for a few hours were assumed to be stable. The only successful surfactant mixture for the preparation of stable W/O emulsion was Span 80-Tween 80 system. The reason was their similar chemical structures which enhanced the interaction of surfactant molecules. It is likely that the lipophilic portion of Tween 80 could easy interact with hydrocarbon tail of Span 80 and form stronger interfacial film.

The surfactant efficiency depends on the amount of surfactant molecules adsorbed at the monomer–water interface. In the case of lipophilic surfactants, this is directly related to the solubility of surfactants in monomer phase. The solubility of each Span 80 and Span 83 in monomer mixture of MMA and EGDMA can be compared by their Hildebrand solubility (δ) parameters. The lower the difference in the value of δ means the higher the miscibility. The solubility parameters were calculated from the formula below.[33]

$$\delta = \sqrt{\frac{\Delta H_{\text{vap}} - RT}{V_m}}, \tag{2}$$

where ΔH_{vap} (J mol^{-1}) is the enthalpy of vaporization, R (J mol^{-1} K^{-1}) the gas constant, T (K) the temperature, and V_{m} (m^3/mol) the molar volume. The ΔH_{vap} values were estimated by the Hildebrand and Scott equation given by[33,34]

$$\Delta H_{\text{vap}} = -12340 + 99.2\, T_b + 0.084\, T_b^2, \tag{3}$$

where T_b is the boiling temperature. The calculated δ values were given in Table II. As seen from Table II, MMA and EGDMA have very close solubility parameters and thus they are compatible and miscible with each other. On the other hand, the Δ value of Span 80 is lower than that of Span 83. It simply means that Span 80 is more compatible with the monomers than with Span 83.

Effect of Hydrophilic-Lipophilic Balance (HLB) Value on the Stability of Emulsion

A set of experiments were performed at different Span 80/Tween 80 ratios to investigate the effect of surfactant mixture on W/O emulsion stability and on water droplet size. This ratio was arranged in a way to set the HLB value to 5, 6, 7, 8, and 9. The ratios of binary surfactant mixtures were given in Table III. The monomer/surfactant/water (M/S/W) weight ratio was kept constant at 66/20/14. The emulsification was performed by ultrasonication at 60 W for 6 min.

The size of water droplets was measured at 0, 6, 12, 18, and 24 h, and the change in the size of water droplets with time was taken as a criterion for the stability of W/O emulsions. The results of size measurements were given in Figure 4. The increase in the HLB value caused a decrease in the average diameter of droplets. This must be due to higher stability achieved at high HLB values.

The low HLB values (i.e., HLB5 & HLB6) exhibited larger fluctuations in particle size. The Ostwald ripening and the coalescence grow the droplet size in time, and the sedimentation of big droplets results in size reduction in the emulsion. According to the Lifshitz-Slezov and Wagner (LSW) theory there is a linear relationship between r^3 (i.e., droplet volume) and time when the dominating breakdown mechanism is Ostwald ripening.[22,35–37] If the relation between $1/r^2$ and time also follows a linear behavior then the prominent instability is coalescence.[22,37] A plot of $1/r^2$ and r^3 versus time was given in Figure 5(a,b). A linear behavior can be assured by R^2 values which are given below the symbols in both figures. It is seen that the R^2 values are quite low to assure linearity. So it can be said that neither the Ostwald ripening nor the coalescence alone is the only driving breakdown of the emulsions studied. As figured out from the fluctuation of droplet size with time, the Ostwald ripening, the coalescence, and the sedimentation are all effective in the breakdown of emulsions.

Table II. The Calculated Solubility Parameters of Monomers and Lipophilic Surfactants

Compound	Solubility parameter (δ)	$\Delta(\delta_{\text{MMA}}\text{-}\delta_2)$
MMA	20.9	
EGDMA	19.8	1.1
Span 80	18.2	2.7
Span 83	14.2	6.7

Table III. Surfactant Ratios at Given HLB Values

Sample	Span 80-Tween 80 (% w/w)
HLB 5	93:7
HLB 6	84:16
HLB 7	75:25
HLB 8	65:35
HLB 9	56:44

As seen from Figure 4 higher droplet sizes favored the sedimentation as expected. In HLB = 5 case, an increasing trend in size in time is observed which may be caused by higher coalescence or Ostwald ripening rate. On the other hand for HLB = 6, the size of droplets reduced in time that may be caused by high sedimentation rate of large droplets. When the HLB value is increased, it was observed that the size fluctuation reduced dramatically. The decrease of size fluctuations in time for high HLB cases indicates that the interaction of particles to yield size growth and sedimentation decreases, and the emulsion achieves higher stability.

The surfactant mixtures with HLB value of 8 and 9 both yielded better stability and smaller droplet. The increase of hydrophilic character with the increase of HLB value can take the system closer to the instability border due to phase inversion of W/O to O/W. This effect may cause destabilization in W/O/W emulsion, and so, in the proceeding experiments the surfactant mixture with an HLB value of 8 was used rather than 9.

Phase Stability Diagram for W/O Emulsion

The amount of the emulsion components, i.e., monomer, surfactant, and water have significant influence on stability and size. The emulsions were prepared with various ratios of monomer, surfactant, and water (M/S/W), and the stability regions of compositions were investigated. For this purpose a ternary phase diagram was prepared to visualize the stable region. In this diagram every point represents a ternary ratio of M/S/W. The W/O emulsions were prepared with Span 80 and Span 80-Tween 80 (HLB 8) surfactant(s), and homogenized by ultrasonic mixing. The phase diagram for W/O emulsions for MMA:EGDMA (1:1) monomer mixture was given in Figure 6.

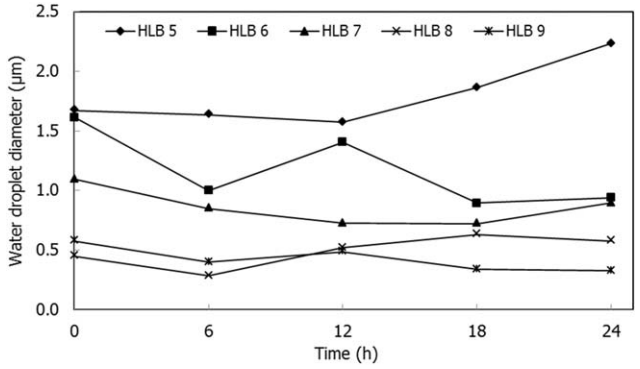

Figure 4. Influence of the HLB value of the surfactant mixture on the size of water droplets.

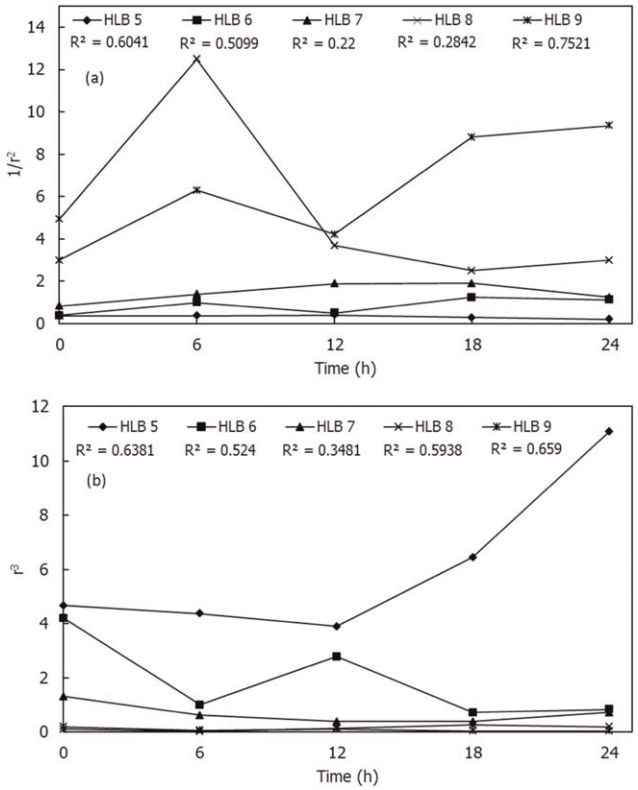

Figure 5. Change of (a) $1/r^2$ and (b) r^3 with time.

It is seen from Figure 6 that the stability region is very small (open triangles) when Span 80 was used alone; but a larger stability region was obtained with Span 80-Tween 80 mixture (open circles). Therefore, it is much advantageous to work with Span 80-Tween 80 mixture.

Effect of Water Content

The amount of water is another parameter that affects emulsion stability. High water concentrations destabilized W/O emulsions due to catastrophic phase inversion which occurs when the amount of water far exceeds the amount of monomer. It was observed in experiments that, when water concentration exceeded 30% w/w, the viscosity of W/O emulsion with a

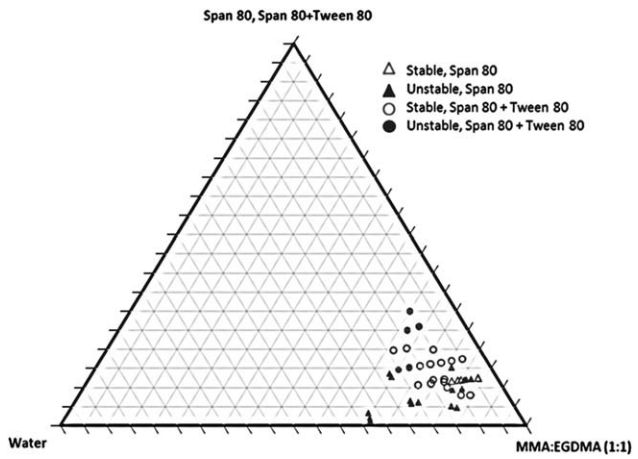

Figure 6. Phase diagram for monomer/surfactant/water system.

surfactant to water weight ratio of 0.125 increased drastically and turned into a viscous phase.

On the other hand, the number of water droplets dispersed in monomer mixture might be increased as the concentration of water increased. This is a desired situation since the higher number of droplets raises the possibility of the existence of multiple droplets inside the W/O/W emulsion. The number of water droplets and the emulsion stability can be optimized by adjusting the process parameters.

Effect of Ultrasonication Parameters on W/O Emulsion Droplet Size

The droplet size is the key factor that determines the diameter of voids inside the hollow polymer particles where water droplets turn into voids in the final step. In order to produce submicron size fine droplets it is necessary to apply sufficiently high force onto monomer–surfactant–water mixture. In the literature, it was reported that very fine droplets could be obtained within very short times by ultrasonication.[38–40] When an ultrasonic wave which has a frequency higher than 20 kHz is imposed on a liquid medium, it created alternating positive and negative pressures in that liquid. The positive and negative pressures cause the liquid molecules to compress and stretch, respectively. When the negative pressure generated by ultrasonic wave is large enough to alter the molecular interactions of liquid, local break down of liquid occurs and voids are generated. These voids are referred as cavitation bubbles. The formation and collapse of those bubbles due to pressure fluctuations generates high energy waves and results in mechanical mixing effect.[38,41]

Effect of Ultrasonication Power

In Figure 7, the effect of ultrasonication power on W/O emulsion droplet size was given. All emulsions were prepared with the same monomer/surfactant/water ratio of 75.5/9.4/15.1, and ultrasonicated for 30 seconds at various mixing powers. It is seen from Figure 7 that minimum droplet diameter was achieved at 80 W. Further increase of power increased the size of water droplets. At high powers the droplets may gain high kinetic energies and hit each other with high momentum. At such powerful collisions, the steric repulsion of interfacial films may be overcome and droplets may coalesce yielding larger size droplets.

Effect of Ultrasonication Time

The duration of ultrasonication on W/O emulsion droplet size was shown in Figure 8. The emulsions were sonicated at 80 W for various mixing times. The ratio of monomer/surfactant/water was taken to be 75.5/9.4/15.1. A similar trend which is seen in Figure 7 was also observed in the ultrasonication time studies. Small droplets formed at short times, and they coalesced with each other and yielded large size particles on prolonged ultrasonication. The fluctuating behavior may be interpreted as the evidence of competition between droplet fragmentation and coalescence.

The energy loaded during ultrasonication increased the temperature of the medium significantly. The temperature rise during ultrasonication at 80 W was illustrated in Figure 9. There is

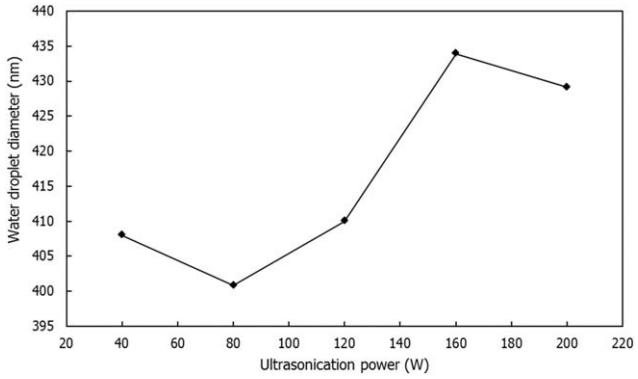

Figure 7. Effect of ultrasonication power on the W/O emulsion droplet size.

almost a linear dependence of the increase of temperature on the time (or total energy) of ultrasonication. In order to avoid undesired loss of monomer mass and phase inversion, all the ultrasonic emulsifications were performed in a cold water bath.

Mathematical Modeling of Scattering Efficiency

Opacity of a pigment is directly dependent on its light scattering ability. The proper hollow size that gives higher opacity can be worked out by a mathematical model which utilizes the Mie scattering efficiency. The extinction efficiencies of hollows for the range of visible incident radiations were calculated by using the formulation of Bohren and Huffman.[7] An efficiency calculation program was written in MATLAB for this purpose by modifying the Bohren and Huffman's formulation and the Matzler's study.[42] The calculations and codes were described in detail in a previous study of Asmaoğlu.[43]

The Bohren and Huffman's scattering efficiency solution is valid for isotropic and spherical single particles where multiple scattering effects are not considered. The calculations in the current study were done by assuming that the medium contains voids embedded in polymer matrix. The scattering efficiencies for various radiations and hollows having diameter in the range of 50–4000 nm were shown in Figure 10.

It seen from Figure 10 that the scattering efficiency has an oscillating behavior, but the amplitude becomes more damped as the diameter of hollows increases. On the other hand, as the wavelength of radiation increases the peaks get wider. The scattering efficiency is measured in terms of the amplitudes of

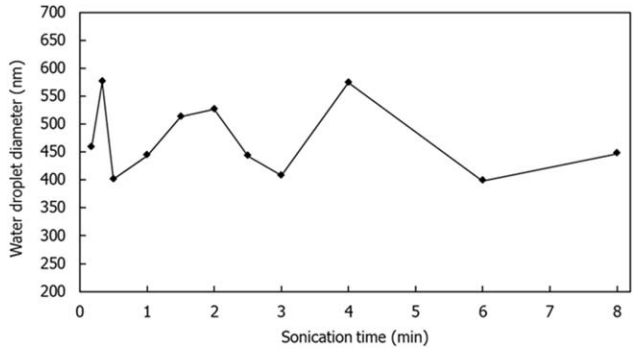

Figure 8. Effect of time of ultrasonication on W/O emulsion droplet size.

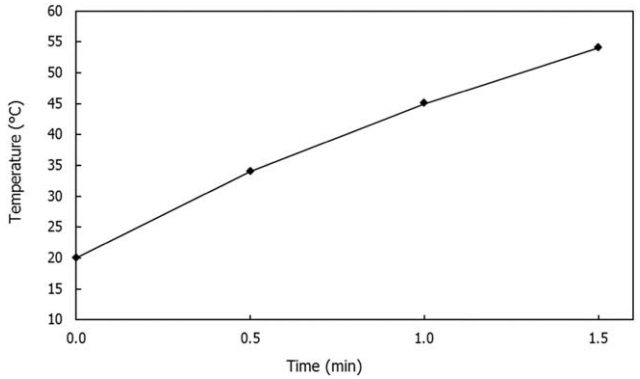

Figure 9. Temperature rise due to the ultrasonication.

peaks. It is seen that the second peak from the beginning (i.e., the right hand side) has the highest amplitude and thus highest scattering efficiency. The subsequent peaks have slightly decreasing scattering efficiencies.

Another observation that can be noticed is that the radiations at different wavelengths have highest efficiency responses at different void sizes. The radiations of visible spectrum with smaller wavelengths are more effectively scattered by relatively smaller voids. Similarly, as the wavelength of radiation increases, the size required for maximum scattering efficiency also increases. This can be easily noticed from the shift of peaks with the increase of hollow diameter. Light interacts with matter as a beam of radiations at various wavelengths. Thus, the mathematical model shows that the voids with a size distribution within the range of wavelengths of visible radiation spectrum and close to 1250 nm size may yield higher scattering performance than single-size voids.

W/O Emulsion Preparation with Required Droplet Size

The previous experiments have shown that smaller droplets could be obtained with ultrasonic homogenization at 80 W for 30 s as mentioned above. In order to generate droplets within the size range of visible spectrum radiations, numerous M/S/W ratios were tested for the W/O emulsification at 80 W and for 30 s. The optimum result was obtained with an M/S/W weight

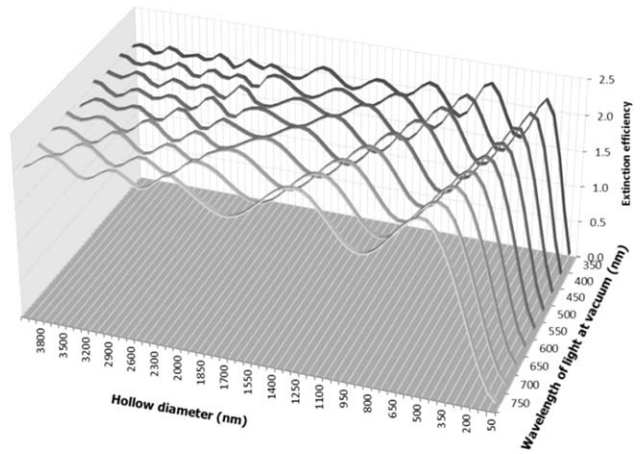

Figure 10. The calculated scattering efficiency profiles of hollows at different diameters and at varying incident radiations.

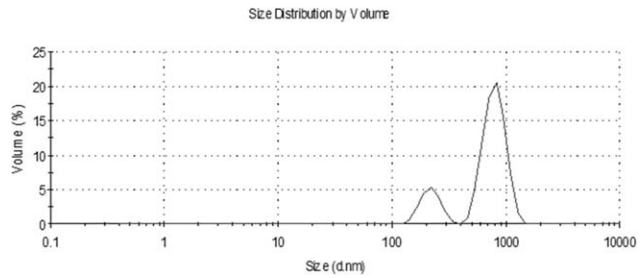

Figure 11. Droplet size distribution of W/O emulsion (M/S/W: 75.5/9.4/15.1), 80 W, 30 s.

ratio of 75.5/9.4/15.1, and with the Span 80-Tween 80 surfactant mixture having an HLB value of 8. The volume size distribution of this appropriate W/O emulsion was given in Figure 11.

Effect of Hydrophilic Surfactant Concentration on W/O/W Emulsion Droplet Size

The prepared W/O emulsions were slowly poured into an aqueous solution of hydrophilic Triton X-405 under mechanical mixing at 1000 rpm for 4 min. In this step, the monomer phase containing water droplets was encapsulated and the spherical monomer droplets with multiple water droplets inside were obtained. In order to investigate the effect of surfactant concentration on monomer droplet size, the W/O/W emulsions were prepared at the surfactant concentrations of 2, 3.5, and 5% w/w. As seen from Figure 12, the increased surfactant concentration reduced the size of droplets.

The images of the prepared multiple emulsions obtained from an optical microscope were given in Figure 13. The images clearly show that the successful preparation of the multiple emulsions with multiple water droplets was accomplished. Nevertheless, there were few W/O/W droplets containing single water droplet inside (see "1" in Figure 13b). There are also a few regular oil-in-water (O/W) droplets (see "2" in Figure 13b).

The W/O/W emulsions were then stabilized by an aqueous solution of 1% w/w polyvinylpyrrolidone. The mixing has to be done at low rpm not to break down the existing morphology of droplets. The comparison of both curves in Figure 12 shows that there is not much change of size during stabilization when

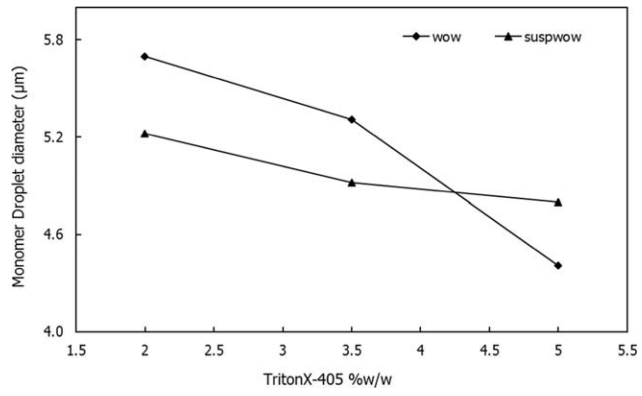

Figure 12. The effect of surfactant concentration on W/O/W emulsion droplet size. (wow: droplet size of the W/O/W emulsion, suspwow: the size of suspended and stabilized droplets of W/O/W emulsion).

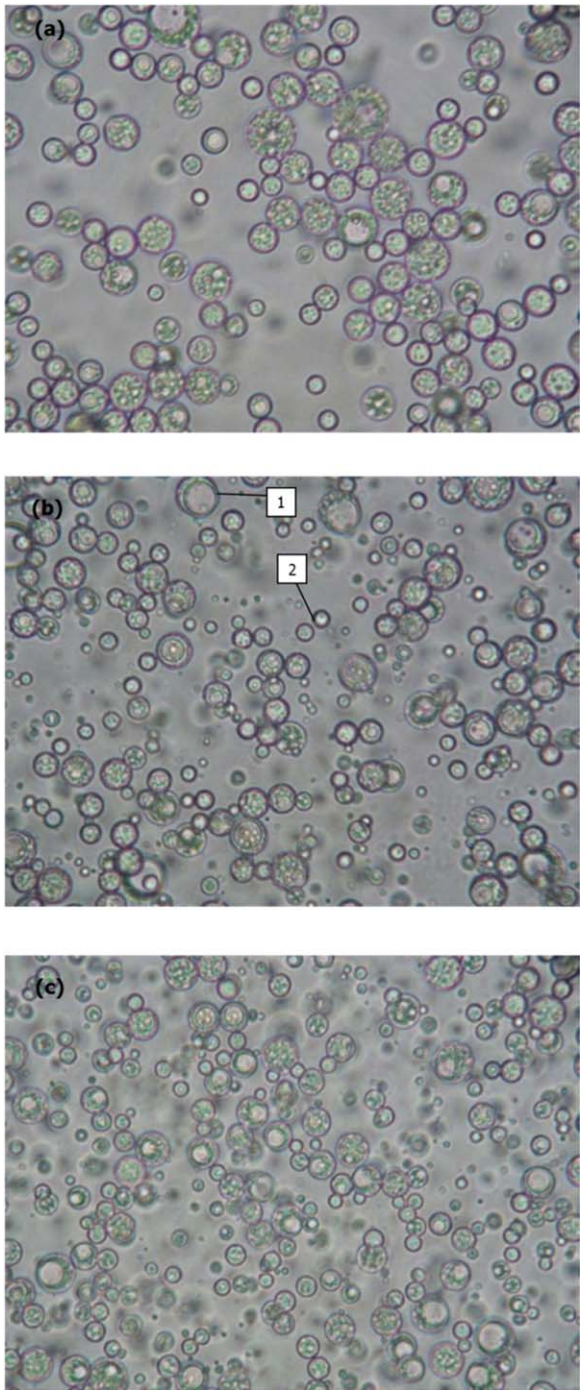

Figure 13. Optical microscopy images for (a) 2% w/w, (b) 3.5% w/w, and (c) 5% w/w, Triton X-405, (×400). [Color figure can be viewed in the online issue, which is available at wileyonlinelibrary.com.]

mixed at 500 rpm for 1 min. The stabilization was done without significantly disturbing the W/O/W emulsion structure. All the proceeding experiments were carried out by using the aqueous solution of 5% w/w Triton X-405.

Effect of Mixing Speed on W/O/W Emulsion Droplet Size

Since the opaque polymer pigment particle was obtained by suspension polymerization of W/O/W emulsion, its size was equivalent to the W/O/W emulsion monomer droplets. Figure 14 shows the effect of mixing speed on the W/O/W emulsion droplet size. The emulsions were mixed for 4 min. As expected, the increase of the mixing speed reduced the diameter.

The reduced size of monomer droplets caused a decrease in the number of multiple droplets as expected. The optimum monomer droplet size having multiple water droplets were obtained in Figure 15b where the mixing was carried at 1250 rpm. Hence the proceeding experiments were performed at 1250 rpm. Ultrasonication was also used as an alternative mixing method in the preparation of multiple emulsions but multiple emulsions could never be obtained even at the very low power of 10 W; only O/W emulsion formed all the time.

Morphology of Opaque Polymer Pigments

The polymer particles were produced by free radical polymerization of the W/O/W multiemulsion. The polymerization reaction temperature was kept as low as possible in order to avoid phase inversion of surfactants. The other concern was the vapor pressure of W/O/W emulsion inner water phase where increased pressure might blast water droplets. The polymerization reactions were performed at 55 °C for 20 h. The morphology of produced opaque polymer pigments and the effects of parameters on hollow structure were investigated by using SEM and TEM. The compositions of the opaque pigments examined were given in Table IV.

The surface morphology of particles was investigated by SEM analysis (Figure 16). As observed from the micrographs, all the polymer particles had polydispersed spherical structure.

The particles have a rough surface which may be due to high degree of crosslinking. The excessive crosslinking increases the porosity of polymer network systems. The very small particles formed between the large ones may have either single hollow or no hollow as mentioned previously (see Figure 15). The multihollow structure of polymer pigment is clearly seen in the SEM micrograph of an OP2 particle (Figure 16b). It is seen that quite large voids also formed which might be caused by the coalescence or Ostwald ripening of the water droplets at early stages of polymerization.

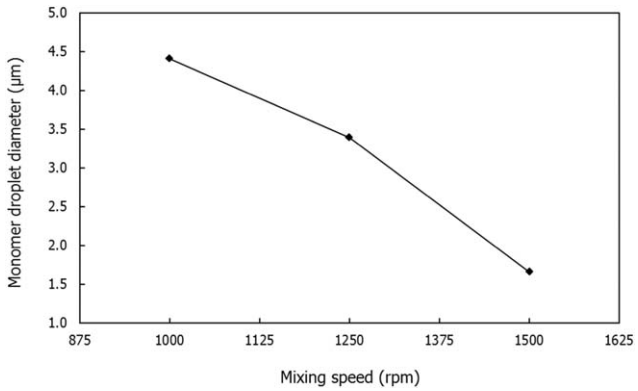

Figure 14. Effect of mixing speed on W/O/W emulsion monomer droplet size.

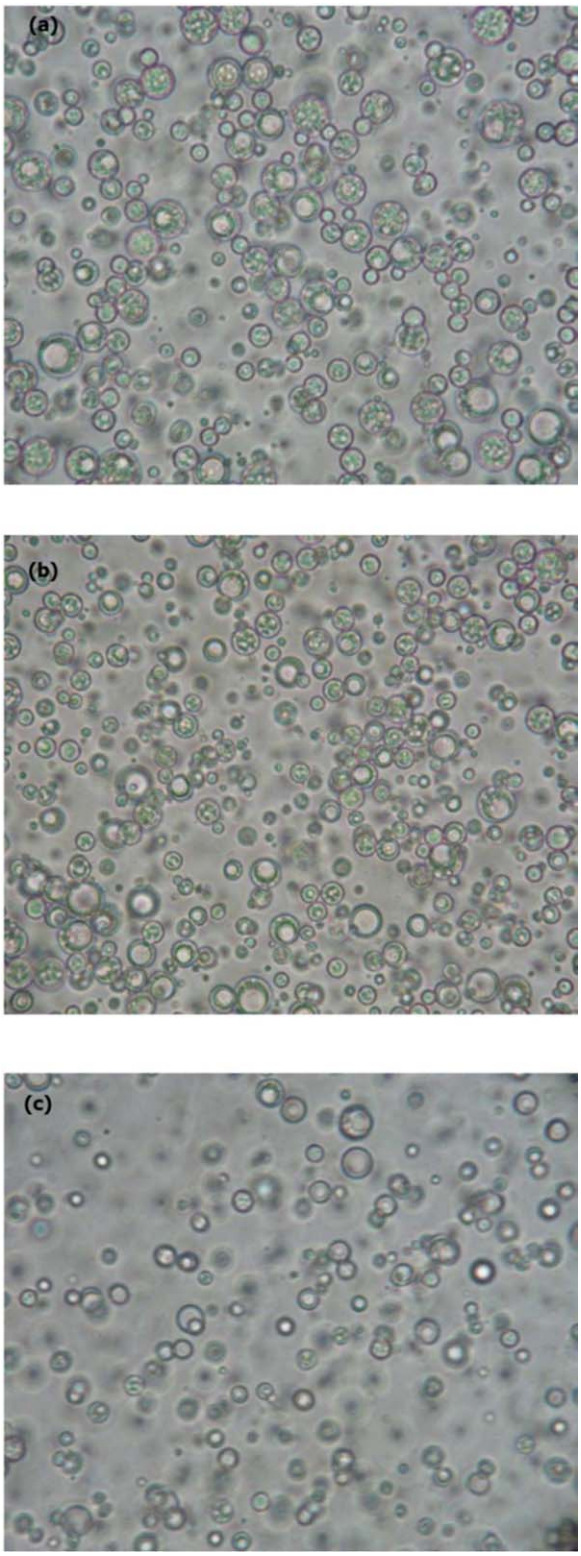

Figure 15. Optical microscopy image of W/O/W emulsions mixed at (a) 1000 rpm, (b) 1250 rpm, and (c) 1500 rpm. (×400). [Color figure can be viewed in the online issue, which is available at wileyonlinelibrary.com.]

Effect of the Inner Water Phase Ratio

The amount of water has significant effect on the stability of both W/O and W/O/W emulsions; it, in turn, affects the hollow structure of polymer particle. Voids (i.e., water droplets) can be captured inside the emulsions only if stability can be persistently accomplished. The previous stability results showed that the large amounts of water destabilized the W/O emulsion. On the other hand, the number of hollows increases with the increase of water/monomer ratio. In order to investigate the effect of water on hollow polymer structure, the W/O/W emulsions were prepared at different water (encapsulated)/monomer ratios of W/O emulsions.

In order to confirm the existence of voids inside the particles and examine the influence of water on hollow structure the TEM analysis was performed. In fact, the micron size particles are not appropriate samples for TEM analysis where relatively high thickness prevents the transmission of electrons. However, the presence of voids inside the particle lowers the wall thickness and makes possible to observe the voids by contrast difference. The TEM micrographs of OP1, OP2, and OP3 were given in Figure 17. The lighter zones in these micrographs are hollows existing inside.

The TEM micrographs indicate that the number of voids per particle increased with the increase of the amount of water. This can be clearly seen from the comparison of OP2 (w/m = 0.2) with OP1 (w/m = 0.1). The number of the multi-hollows in OP2 is much more than the one in OP1. In fact OP1 is dominated by single hollows while each particle in OP2 contains several hollows. On the other hand, further increase in the amount of water lowered the number of hollows as seen from OP3 (w/m = 0.3). The reason was the decreased W/O/W emulsion stability due to the excess amount of water in W/O emulsion in this case.

Effect of Surfactants Used in W/O Emulsion

The TEM micrographs of OP4 and OP5 were given in Figure 18, where, OP4 and OP5 had the surfactant (Span 80-Tween 80) mixture to monomer phase [MMA:EGDMA (1:1)] ratio of 0.075, and 0.175, by weight, respectively.

Table IV. Compositions of Opaque Pigments

Sample	s/m[a]	w/m[b]	Thickener[c] (% w/w)
OP1	0.125	0.1	
OP2	0.125	0.2	
OP3	0.125	0.3	
OP4	0.075	0.2	
OP5	0.175	0.2	
OP6	0.125	0.2	0.25
OP7	0.125	0.2	0.5
OP8	0.125	0.2	1.0
OP9	0.125	0.2	1.5

[a] Weight ratio of Span 80-Tween 80 (HLB 8) to monomer phase MMA:EGDMA (1:1).
[b] Weight ratio of water to monomer phase MMA:EGDMA (1:1).
[c] Percent weight ratio of thickener (polystyrene) in monomer phase.

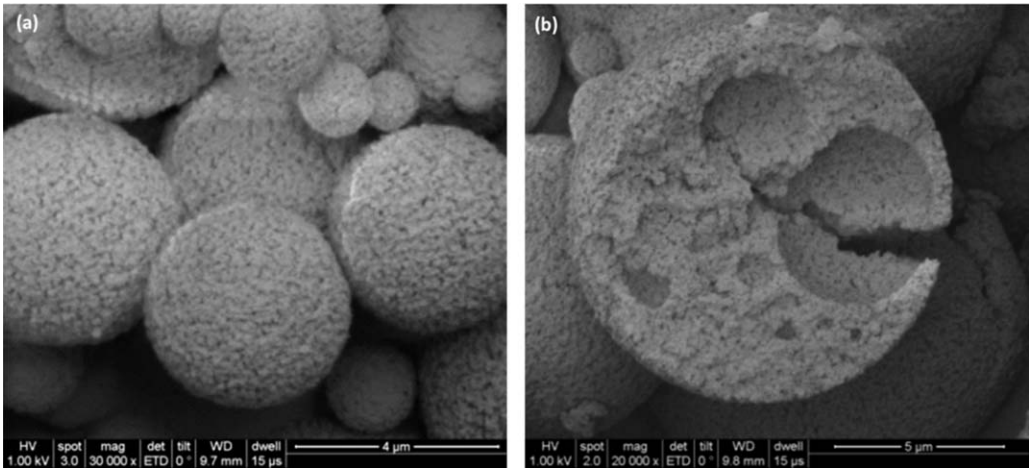

Figure 16. SEM micrographs of (a) OP1 and (b) OP2.

OP5 has larger number of multihollows than OP4 as seen from the last micrograph. The reason is thought to be the increased interfacial film strength of the W/O emulsion with higher amount of surfactant molecules which provided higher stability.

Effect of Thickener

In this study, a thickening agent was also used to enhance the W/O/W emulsion stability by increasing the viscosity of monomer phase. The increase of viscosity is expected to lower the Ostwald ripening. In order to increase viscosity, the solution of polystyrene (PS) in methyl methacrylate (10% w/w) was prepared and added to the monomer phase. PS dissolved more easily than polymethyl metacrylate in methyl methacrylate monomer, therefore PS was preferred for use as thickener. The viscosity change of solution with the amount of PS in monomer mixture was shown in Figure 19.

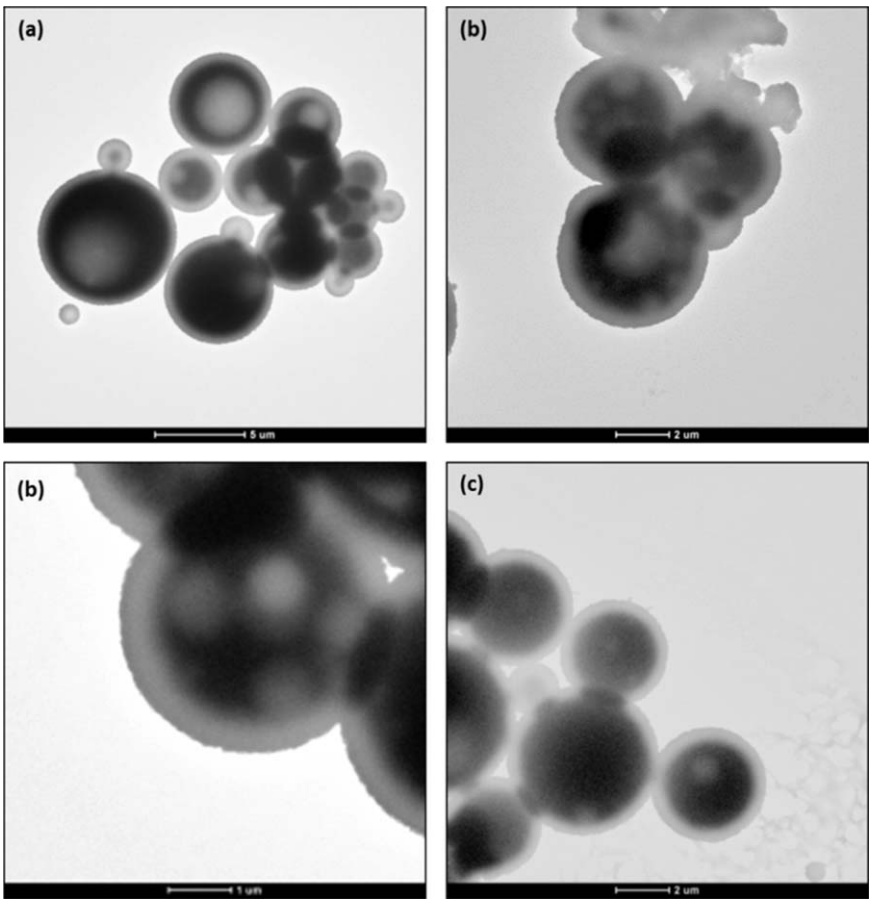

Figure 17. TEM micrographs of (a) OP1 (w/m = 0.1), (b) OP2 (w/m = 0.2) (two different magnifications), and (c) OP3 (w/m = 0.3).

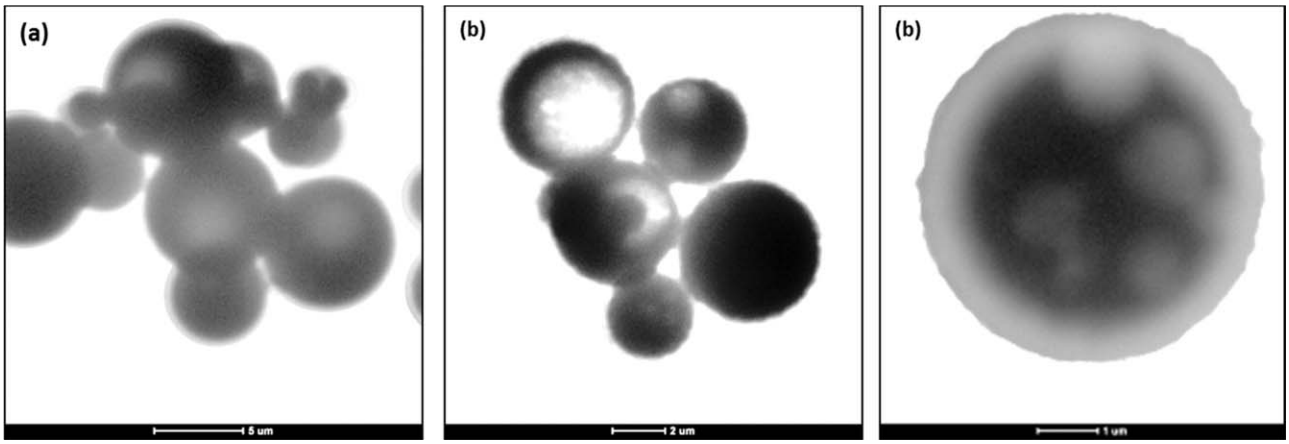

Figure 18. TEM micrographs of (a) OP4 (s/m = 0.125) and (b) OP5 (s/m = 0.175) (two different magnifications).

In heterogeneous systems having liquid droplets or bubbles with varying sizes, the stability cannot be easily accomplished. This is because of the surface dependent forces developed as considered in the Kelvin equation or in the Gibbs-Thomson equation. The decrease of the radius increases these forces or surface potentials, and small bubbles or droplets coalesce into big bubbles (i.e., Oswald ripening). Decreasing the vapor pressure may reduce and even eliminate the Oswald ripening. Adding PS into the medium naturally decreases the vapor pressure according to the Raoult's law as PS has practically zero vapor pressure. At large quantities of PS the cohesive forces in the heterogeneous medium and thus the resulting surface tension forces increased to such an extent that the multihollow configuration was adversely influenced.

The TEM micrographs of the synthesized polymer pigments OP6, OP7, OP8, and OP9 having PS were given in Figure 20. As observed from the TEM micrographs, the multihollow structured particles were also obtained when the PS content was low [Figure 20(a,b), i.e., OP6 and OP7 cases]. The high amounts of PS adversely affected the morphology as seen from Figure 20(c,d).

Opacity Measurements

The opacity and the hiding power depend on the scattering ability of hollow polymer particles. The voids act as scattering centers and deviate the direction of incident visible light. The opacity of the polymer pigments is dependent both on the size of voids and on the number of hollows inside the particles. The opacity measurements of synthesized polymer pigments were given in Table V, where the opacity of TiO_2 was given in the last column for comparison.

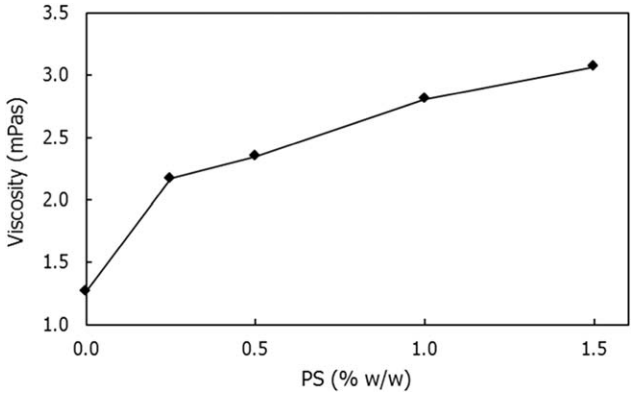

Figure 19. Effect of PS concentration on the viscosity of MMA:EGDMA (1:1) mixture.

The results show that the particles OP2, OP5, and OP6, which have high number of multihollows, have highest opacities. The existence of multiple voids inside a particle increase the number of polymer–air interface and create multiple scatterings that results in higher diffraction.

Another property which influences the extent of opacity is the surface morphology of particles. Opacity increases with the increase of surface roughness, because, roughness generates different angles of reflections, i.e., it increases the diffraction and thus the fraction of diffuse light.

Effect of the Amount of Pigment on Paint Opacity

A commercial paint contains about equal volumes of resin and pigment. In order to determine the effect of hollow polymers synthesized on the opacity of paint, the hollow pigments were introduced into water based styrene-acrylic resin. The change of opacity with the amount of added hollow pigment was given in Figure 21. The opacity increases with the amount of pigment loaded. For comparison the opacity change with TiO_2 was also given in Figure 21.

At 50% loading the opacity of polymer pigment and TiO_2 became almost equal. In the industry unless high gloss is needed relatively cheaper pigments and extenders with relatively low gloss such as calcite ($CaCO_3$) and baryte ($BaSO_4$) are used in paints. So the multihollow polymer pigments can be a good substitute for such low gloss pigments and extenders.

Gloss Measurements

The results of the specular gloss measurements at incident angles of 20, 60, and 85° were given in Table VI.

The very low gloss values actually are due to the very high opacity and porous structure of pigments synthesized. The gloss value of paint can be described as the angle dependent measure of the relative ratio of diffused reflection to specular reflection

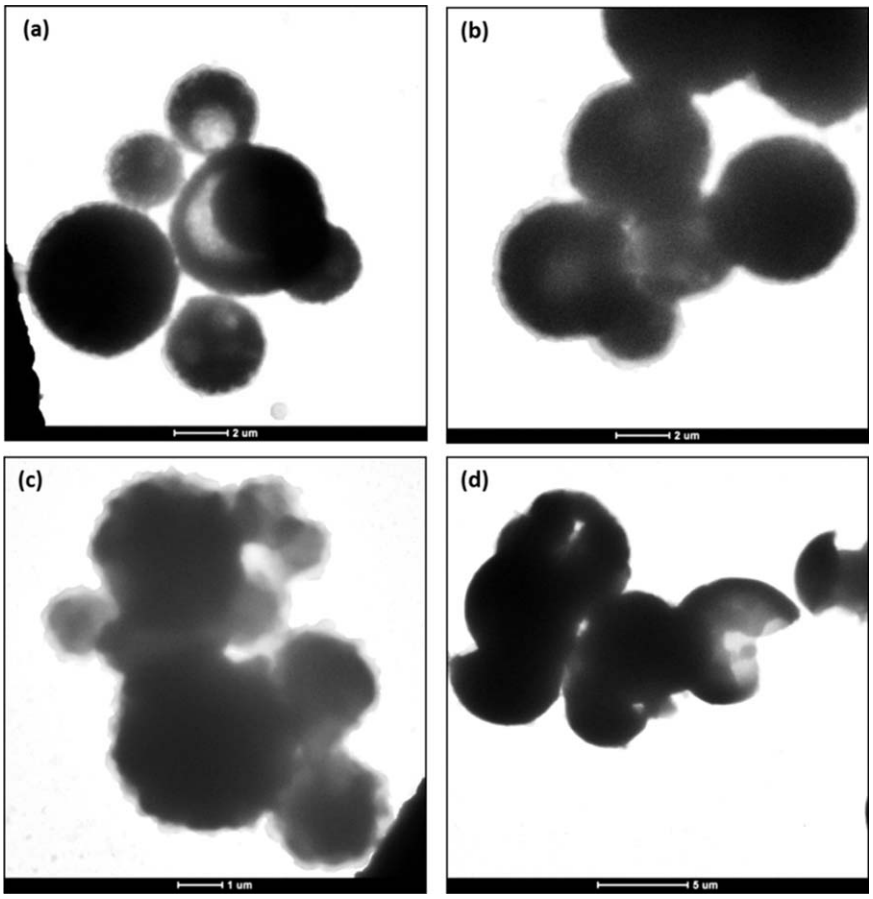

Figure 20. TEM micrographs of (a) OP6 (0.25% w/w), (b) OP7 (0.5% w/w), (c) OP8 (1% w/w), and (d) OP9 (1.5% w/w).

from the surface. The incident light angles of 20, 60, and 85° are used to define high gloss, medium gloss, and matte paints, respectively. A value lower than 10 indicates matte surface and higher than 70 indicates high gloss. Table VI indicates that the pigments synthesized all have very low gloss values.

Table V. Opacities of Polymer Pigments

Pigment	OP1	OP2	OP3	OP4	OP5
Opacity	87.6	93.9	90.8	78.9	97.3
Pigment	OP6	OP7	OP8	OP9	TiO_2
Opacity	96.1	91.9	87.0	82.3	100

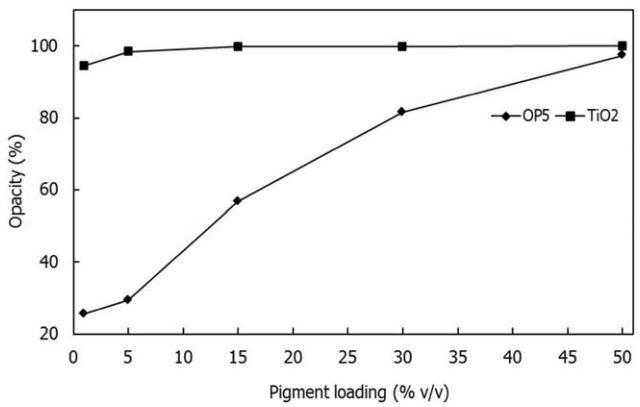

Figure 21. Effect of pigment concentration on paint opacity.

*L*a*b* Color Measurement

The *L* value indicates the lightness of sample and it is 0 for black and 100 for pure white. On the other hand, *a* value is the measure of color from red to green (+ means shift to red and – means shift to green), and *b* from yellow to blue (+ means shift to yellow and – means shift to blue). The dE^* shows the

Table VI. Gloss Values of Opaque Polymer Pigments

Sample	20°	60°	85°
OP1	1.9	2.9	1.6
OP2	1.9	2.7	3.0
OP3	1.8	2.7	1.5
OP4	1.8	3.0	2.3
OP5	1.9	2.6	2.5
OP6	1.8	2.6	1.9
OP7	1.9	2.8	1.6
OP8	1.8	2.6	0.8
OP9	1.9	2.9	1.2
Resin[a]	137.7	133.2	110.9

[a] Styrene-acrylic resin free of pigment.

Table VII. The Color Properties of Opaque Polymer Pigments Compared to TiO_2

Sample	dL^*	da^*	db^*	dE^*
OP1	−18.93	0.86	−1.92	19.05
OP2	−9.49	0.53	−2.22	9.76
OP3	−15.17	0.82	−1.91	15.31
OP4	−19.00	1.27	0.46	19.05
OP5	−8.38	0.44	−1.78	8.58
OP6	−11.26	0.30	−2.47	11.53
OP7	−15.79	0.75	−1.38	15.87
OP8	−20.27	1.06	−0.09	20.30
OP9	−28.96	1.25	0.48	28.99

Euclidean distance in color space.[44,45] In Table VII the color deviations of synthesized opaque polymer pigments were given when rutile TiO_2 was taken as the reference.

As seen from Table VII, the opaque pigments OP2 and OP5 (which have low dL^* values) have more close lightness and less total color difference (dE^*) to TiO_2 than the others. The dE^* gives information about how much the pigment examined deviates from the reference pigment in color properties. The shift of color to blue might be caused by the existence of polymer particles having diameters lower than 100 nm. Below this diameter, particles make more Rayleigh scattering which inversely changes with the fourth power of the wavelength of radiation. That is, blue component of visible light undergoes more scattering and starts to dominate the overall spectrum, and the color shifts to the blue side.

CONCLUSIONS

The mixture of "Span 80-Tween 80" surfactants provided better emulsion stability than "Span 80-only" for W/O emulsion. The surfactant mixture with the HLB values of 8 yielded better stability, and lowered the water droplet size.

The optimum diameters of voids for high scattering efficiency were predicted by a mathematical model using the Mie scattering. Voids having a size distribution ranging within the wavelength of visible spectrum radiations are more effective than single-size voids for light scattering.

The W/O/W emulsion was prepared by the dispersion of the W/O emulsion in aqueous solution of hydrophilic surfactant Triton X-405. The increase of surfactant concentration, mechanical mixing speed, and time had reducing effect on the monomer droplet size of the W/O/W emulsion. The optimum size for the monomer droplet which then formed polymer particles was obtained at 1250 rpm mixing for 4 min.

High degree of crosslinking due to EGDMA resulted in porous structure and rough surface. The increase of the viscosity of monomer phase due to the use of a thickener (in this study, PS) slightly enhanced the double emulsion stability. However, further increase in viscosity had destructive effect on voids and on particle sphericity. The produced polymer pigments provided 97.3% opacity at 50% v/v without any other additive. The polymer pigment particles had very low gloss (very high opacity).

ACKNOWLEDGMENTS

This work was supported by TÜBİTAK (Turkish Scientific and Technical Research Council) under the contract number 110T768, and also by Orta Doğu Teknik Universitesi (Middle East Technical University) under the contract number BAP-03-04-2011-001.

REFERENCES

1. Itou, N.; Masukawa, T.; Ozaki, I.; Hattori, M.; Kasai, K. *Colloid Surf. A* **1999**, *153*, 311.
2. McDonald, C. J.; Devon, M. J. *Adv. Colloid Interface Sci.* **2002**, *99*, 181.
3. Jin, L.; Xu, Q. *Adv. Mater. Res.* **2013**, *652–654*, 740.
4. Narongthong, J.; Nuasaen, S.; Suateewong, T.; Tangboriboonrat, P. *Colloid Polym. Sci.* **2015**, *293*, 1269.
5. Mishchenko, M. I. *J. Quant. Spectrosc. Radiat. Transfer* **2009**, *110*, 1210.
6. Helmuth, H.; Quant, J. *Spectrosc. Radiat.* **2009**, *110*, 787.
7. Bohren, C. F.; Huffman, D. R. In Absorption and Scattering of Light by Small Particles, Wiley-VCH Verlag GmbH: New York, **2007**; pp 82–129.
8. van de Hulst, H. C. Light Scattering by Small Particles, John Wiley & Sons: New York, **1957**.
9. Kowalski, A.; Vogel, M. (Rohm and Haas Co.). U.S. Pat. 4,427,836 (**1984**).
10. Kowalski, A.; Vogel, M. (Rohm and Haas Co.). U.S. Pat. 4,469,825 (**1984**).
11. Deng, W.; Wang, M. Y.; Cheng, G.; Kan, C. Y. *Eur. Polym. J.* **2010**, *46*, 1210.
12. Khan, A. K.; Ray, B. C.; Dolui, S. K. *Prog. Org. Coat.* **2008**, *62*, 65.
13. Matsumoto, S. *Am. Chem. Soc.* **1985**, *272*, 415.
14. Q. X.;, L. Wang, J.; Zhu, *J. Pharm. Sci.* **2011**, *100*, 2203.
15. Florence, A. T.; Whitehill, D. *Int. J. Pharm.* **1982**, *11*, 277.
16. Masahiro, N. *Adv. Drug Delivery Rev.* **2000**, *45*, 1.
17. Vasudevan, T. V.; Naser, M. S. *J. Colloid Interf. Sci.* **2002**, *256*, 208.
18. Rosen, M. J. Surfactants and Interfacial Phenomena; Wiley: New York, **1978**.
19. Somasundaran, P.; Farinato, R.; Metha, S. C.; Wines, T. H.; Garti, N. in Surfactants in Personal Care Products and Decorative Cosmetics; Rhein, L. D., Schlossman, M., O'Lenick, A., Somasundaran, P., Eds; 3th ed.; CRC Press; **2006**, pp 149–175.
20. Tadros, T. F. Emulsion Science and Technology; Wiley-VCH: Weinheim, **2009**, pp 1–56.
21. Tadros, T. F. Emulsion Science and Technology; Wiley-VCH: Weinheim, **2009**, pp 115–187.
22. Porras, M.; Solans, C.; Gonzalez, C.; Gutierrez, J. M. *Colloid Surf. A* **2008**, *324*, 181.
23. Arai, H.; Shinoda, K. *J. Colloid Interface Sci.* **1967**, *25*, 396.

24. Peng, L. C.; Liu, C. H.; Kwan, C. C.; Huang, K. F. *Colloid Surf. A* **2010**, *370*, 136.
25. Myers, D. Surfactant Science and Technology; Wiley, **2005**, pp 280–322.
26. Zatz, J. L. Encyclopedia of Emulsion Technology; Becher, P. Ed.; Marcel Dekker: New York, **1987**; Vol.*3*.
27. Pellicer, J.; García-Morales, V.; Hernández, M. J. *Phys. Educ.* **2000**, *35*, 126.
28. Song, M. G.; Jho, S. H.; Kim, J. Y.; Kim, J. D. *J. Colloid Interface Sci.* **2000**, *230*, 213.
29. Boyd, J.; Parkinson, C.; Sherman, P. *J. Colloid Interface Sci.* **1972**, *41*, 359.
30. Griffin, W. *J. Soc. Cosmet. Chem.* **1949**, *1*, 311.
31. Griffin, W. *J. Soc. Cosmet. Chem.* **1954**, *5*, 249.
32. Hildebrand, J. H.; Scott, R. L. Solubility of Nonelectrolytes; 3rd ed.; Reinhold: New York, **1950**.
33. Barton, A. F. M. CRC Handbook of Solubility Parameters and Other Cohesion Parameters; 2nd ed.; CRC Press: Baton Rouge, **1983**.
34. Binks, B. P. Modern Aspects of Emulsion Science; The Royal Society of Chemistry Publications: Cambridge, UK, **1998**; pp 1–55.
35. Wagner, C. Z. *Zeitschrift Für Elektrochemie* **1961**, *65*, 581.
36. Porras, M.; Solans, C.; Martinez, A.; Guinart, A.; Gutierrez, J. M. *Colloid Surf. A* **2004**, *249*, 115.
37. Jafari, S. M.; He, Y.; Bhandari, B. *Int. J. Food Prop.* **2006**, *9*, 475.
38. Abismail, A.; Canselier, J. P.; Wilhelm, A. M.; Delmas, H.; Gourdon, C. *Ultrason. Sonochem.* **1999**, *6*, 75.
39. Jafari, S. M.; He, Y.; Bhandari, B. *J. Food Eng.* **2007**, *82*, 478.
40. Lin, C. Y.; Chen, L. W. *Fuel Process. Technol.* **2006**, *87*, 309.
41. Santos, H. M.; Lodeiro, C.; Capelo-Martínez, L. J. In Ultrasound in Chemistry; Wiley-VCH: Weinheim, **2009**, pp 1–16.
42. Matzler, C. MATLAB Functions for Mie Scattering Absorption; Universitas Bernensis, Research report no. 2002-08, **2002**.
43. Asmaoğlu, S. Synthesis and Characterization of Multi-Hollow Opaque Polymer Pigments, M.Sc. Thesis, Middle East Technical University, Ankara **2012**.
44. Hunt, R. W. G.; Pointe, M. R. In Measuring Colour; Wiley: New York, **2011**, pp 41–72.
45. ISO 11664-4:2008(E)/CIE S 014-4/E:2007: Colorimetry - Part 4: CIE 1976 L*a*b Color Space.